Supporting Information

Klumpp and Hwa 10.1073/pnas.0804953105

Methods

Detailed Description of the Model. To partition RNAPs into the 5 classes of our model, we expressed the numbers of RNAPs in each class in terms of measured microscopic quantities as follows.

To express the numbers of RNAPs transcribing mRNA and rRNA, N_m and N_r, we use a Michaelis–Menten model for the activity of the corresponding promoters (1), an average promoter of mRNA-encoding operons and an effective promoter describing the *rrn* promoter pair P1-P2. These promoters are characterized by 2 parameters, their maximal transcription rates (V_m and V_r, respectively) and their Michaelis constant (K_m and K_r). The ratio of these 2 parameters ($A_m = V_m/K_m$ and $A_r = V_r/K_r$) provides a measure of the strength of the corresponding promoter (2). The transcription rate (or frequency of initiation of transcription) depends in addition on the concentration of free RNAPs, c_{free}, and is given by $f_m = V_m\, c_{free}/(K_m + c_{free})$ for each mRNA operon and likewise for rRNA. The numbers of elongating RNAPs per operon are then given by $L_m f_m/c_m$ and $L_r f_r/c_r$, where L_m and L_r are the length of the operons and c_m and c_r are the transcript elongation speeds. To obtain the numbers of elongating RNAPs per cell, these numbers are multiplied by the numbers of operons per cell (N_{rrn} for rRNA and $N_{op} \times G_C$ for mRNA, where N_{op} is the number of different active operons on the genome and G_C is the number of genome equivalents per cell). The total numbers of RNAPs involved in transcription also include promoter-bound RNAPs; the number of those is expressed as the product of the number of operons and the promoter occupation, which in the Michaelis–Menten model is given by f_m/V_m. In summary, we obtain the following expressions for the numbers of RNAPs transcribing mRNA and rRNA

$$N_m = G_C N_{op} f_m [1/V_m + L_m/c_m]$$

$$= G_C N_{op} \frac{c_{free}}{c_{free} + K_m} [1 + L_m V_m/c_m] \qquad \textbf{[1a]}$$

and

$$N_r = N_{rrn} \frac{c_{free}}{c_{free} + K_r} [1 + L_r V_r/c_r] \qquad \textbf{[2a]}$$

In these expressions, the term describing promoter-bound RNAPs is usually small compared with the term describing elongating RNAPs: Even if an RNAP spends on average 50-fold more time at the promoter than at a site within the operon, as suggested by a recent estimate obtained from chromatin immunoprecipitation experiments (3), the promoter-bound RNAPs account only for ≈2% ($50/L_m$ with $L_m = 3{,}000$) of the RNAPs involved in transcription.

A second estimate of the numbers of RNAPs transcribing mRNA and rRNA is obtained from the measured rates of overall mRNA and rRNA synthesis (r_m and r_r) and the elongation speeds (c_m and c_r), which leads to

$$N_n = r_m/c_m \qquad \textbf{[1b]}$$

$$N_r = r_r/c_r \qquad \textbf{[2b]}$$

Nonspecific binding of RNAPs to DNA is modeled as a binding equilibrium with dissociation constant K_{ns}, so that the number of nonspecifically bound RNAPs, N_{ns}, is given by

$$N_{ns} = n_{sites} c_{free}/(c_{free} + K_{ns}), \qquad \textbf{[3]}$$

where $n_{sites} = g\, G_C$ is the number of binding sites, approximated by the product of genome size g and number of genome equivalents per cell, G_C.

The number of RNAPs free in the cytoplasm is given by the concentration of free RNAPs via

$$N_{free} = c_{free} V_C \qquad \textbf{[4]}$$

with the cell volume V_C. Finally, the number of RNAP assembly intermediates is

$$N_{interm} = N_{RNAP}(1 - 2^{-\mu\tau}), \qquad \textbf{[5]}$$

where μ is the growth rate and τ is the maturation time of newly synthesized RNAPs. The latter expression, which has also been used in ref. 4, was derived by assuming that there is a delay of time τ after which a newly synthesized RNAP is fully assembled and functional. This assumption means that only RNAPs that had been there already a time τ earlier are functional. In exponential growth, these RNAPs are a fraction $2^{-\mu\tau}$ of the total RNAPs.

These microscopic expressions for the RNAP numbers in the 5 different fractions are used in 3 steps. We first estimated N_m and N_r by Eqs. **1b** and **2b** and partitioned the remaining RNAPs by solving

$$N_{RNAP} - N_m - N_r = N_{free} + N_{ns} + N_{interm} \qquad \textbf{[6]}$$

for the concentration of free RNAPs, c_{free}, using parameter sets for different growth rates. All parameters needed to solve Eq. **6** are known with the exceptions of K_{ns} and τ, which were determined by fitting the ratio of cytoplasmic RNAP to total RNAP, $(N_{free} + N_{interm})/N_{total}$, to the minicell data (see below and supporting information (SI) Fig. S1). When these parameters are fixed, Eq. **6** leads to the predicted partitioning of RNAPs shown in Fig. 2. Finally, we used Eqs. **1a** and **2a** together with the predicted free-RNAP concentration and estimates of the maximal transcription rate to determine the promoter strengths A_r and A_m.

The resulting promoter strengths for mRNA were used to study RNAP over- and underexpression as well as the stringent response. To study RNAP over- and underexpression, we used Eq. **1a** to describe the transcription of mRNA with the determined Michaelis constant of the mRNA promoters. For the transcription of rRNA, we fixed the number of RNAPs transcribing rRNA to the value for wild-type cells with normal RNAP level to mimic the effect of feedback control. We then varied the total number of RNAPs per cell and determined the partitioning of the remaining RNAPs into the other 4 classes as well as the resulting transcription rate for mRNA. To study the different scenarios for the stringent response, we used the determined promoter strengths both for mRNA and rRNA, and adjusted one or several of the model parameters according to what has been measured during the stringent response.

Parameter Values. All parameter values used in the calculations for balanced exponential growth are summarized in Table S1 and Table S2. Most of these parameter values were taken from tables 3 and 4 of the review by Bremer and Dennis (5). Parameters not given there were estimated in the following way: Numbers of RNAPs transcribing mRNA and rRNA were determined by

using Eq. **2**. The cell volume was calculated from the cell mass by using the cell mass and volume measurements of ref. 6. The dissociation constant of nonspecific binding, K_{ns}, and the maturation time τ of newly synthesized RNAPs were taken to be independent of growth rate and determined by fitting the fraction of RNAP that is cytoplasmic, $(N_{free} + N_{interm})/N_{RNAP}$, to the values measured by using minicells at 1.23 and 2.5 doublings per hour (7, 8), as described below.

The average length of an *rrn* operon is 5,400 nt according to EcoCyc (9); in our model we increased this length to 6,500 nt to account for the remaining tRNA genes that are not in *rrn* operons ("appending" them to the *rrn* operons). The average mRNA transcript has a molecular mass of 10^6 Da (10), which corresponds to an average operon length L_m of ≈3,000 nt, an estimate consistent with an average of 2.6 genes per operon (11) and an average gene length of ≈1,000 nt (12). To determine the Michaelis constants, K_m and K_r, and the promoter strengths (A_m and A_r) of mRNA and rRNA promoters, we took the maximal transcription rates of these operons to be 90 min^{-1} and 10 min^{-1}, respectively. These estimates are based on the highest transcription rates measured in vivo, which are in the range of 70–85 min^{-1} for rRNA and 1.5–25 min^{-1} for mRNA (2, 13), and the theoretically determined limits for the transcription rate (≈90 min^{-1} for rRNA, at most 40 min^{-1} for mRNA; ref. 14). An estimate for the Michaelis constant K_r of the *rrn* promoters during the stringent response has been obtained by extrapolating the predicted growth-rate dependence of the promoter strength (Fig. 4*A*) to a growth rate of zero. This leads to K_r ≈10–20 μM.

Determination of K_{ns} and τ. To determine the 2 unknown model parameters, the dissociation constant K_{ns} for nonspecific binding to DNA, and the RNAP maturation time τ, we used data from minicell experiments (7, 8). In these experiments, the fraction of cytoplasmic RNAPs (N_{cyto}/N_{total}) was measured at two different growth rates: 14% at 1.23 doublings per hour (7) and 17% at 2.5 doublings per hour (8). According to our model, the cytoplasmic RNAP consists of the free RNAP and assembly intermediates, i.e., $N_{cyto} = N_{free} + N_{interm}$. We can thus fix the two parameters by matching the fraction of cytoplasmic RNAP, i.e., $(N_{free} + N_{interm})/N_{total}$, predicted according to our model with chosen values of K_{ns} and τ, to the above results of the minicell experiments (Fig. S1). This procedure leads to a maturation time τ of 3.4 min and a dissociation constant for nonspecific binding of 3,100 μM (Fig. S1*A*). The maturation time τ of 3.4 min is consistent with the appearance of newly synthesized β subunit in the nucleoid after ≈5 min (15), which should include maturation and transition to the nucleoid as mentioned above. Values for the dissociation constants for nonspecific binding measured in vitro depend on ionic conditions and range between ≈1 μM under low-salt conditions and ≈1,000 μM for high-salt concentration supposed to approximate physiological conditions (16) [a higher estimate for low salt has been obtained in another study (17)]. Our estimate for the in vivo value (3,100 μM) is thus consistent with the in vitro results. It is also very similar to a recent in vivo estimate (1,000 μM) of the dissociation constant for nonspecific DNA binding of the Lac Repressor (18).

Additional Discussion

Growth-Rate Dependence of Macromolecular Crowding. In our model, we have assumed that the dissociation constant for nonspecific binding as well as the Michaelis constants of the promoters are not growth-rate dependent. They could be growth-rate dependent, however, if the degree of macromolecular crowding, i.e., the macromolecular volume fraction, were different for cells growing with different growth rates. Changes in the macromolecular volume fraction can both increase or decrease reaction rates and affinities, depending on whether the reaction is transition-state- or diffusion-limited (19). Changes in the concentration of macromolecules have been observed for *E. coli* cells in media with increased osmolarity (20) and changed crowding has recently been proposed to play an important role in strains with reduced number of *rrn* operons (4). Direct measurements of the macromolecular volume fraction for *E. coli*, however, are quite limited for different growth media at fixed osmolarity. Zimmerman and Trach have measured the concentrations of macromolecules (RNA + protein) for *E. coli* grown in rich medium during exponential and stationary phase and found only a small difference between the two situations, with 0.3–0.37 g/ml in exponential growth phase and 0.34–0.4 in stationary phase (21). We expect the difference between exponential growth with different growth rates to be smaller than the difference between fast exponential growth and stationary phase, so these results suggest that macromolecular crowding should be similar at different growth rates. Furthermore very similar diffusion coefficients have been measured for the diffusion of GFP variants in the cytoplasm of cells growing in rich (22) and minimal medium (18), which also suggests that there is no big difference in crowding for different growth rates. (Unfortunately, the two experiments use different GFP variants, but their molecular weights are the same.)

On the other hand, the data for cell mass and volume of ref. 6 (see also Table S1) indicate an increase of the density (mass/volume) over the range of growth rates studied here. It is possible that this increase in density is an artifact of the volume measurements. We therefore checked whether our results are changed if a constant density is used. In that case, we obtain a lower value for the maturation time τ and therefore a smaller fraction of immature RNAPs, but otherwise the results are very similar to those for a growth-rate-dependent density. In particular, the growth-rate dependence of the free RNAP concentration (and thus the predicted transcription rates for constitutive promoters) is almost indistinguishable from the data shown in Fig. 3 (the absolute value of the free-RNAP concentration is, however, slightly larger). We also obtained similar results when we used the cell volume data given by ref. 23; see also the footnote to Table S2. On the other hand, if we assume that the increase in density at faster growth is real, we can estimate an increase in the macromolecular volume fraction from ≈0.24 at 0.6 doublings per hour to ≈0.34 at 2.3 doublings per hour by using the growth-rate-dependent density (mass/volume; Table S1) and macromolecular mass fraction (5) together with the measured macromolecular volume fraction at fast growth (21). This implies that the free volume is decreased by ≈13% at 2.4 doublings per hour compared with 0.6 doubling per hour. In this scenario, the change of macromolecular crowding would lead to an additional increase of the effective concentration of free RNAPs by ≈13% over the range of growth rates studied here, or, equivalently, to a ≈13% decrease of the dissociation constants for both nonspecific binding to DNA and for binding to promoters. This estimate of the effect of increased crowding is small compared with the 2.3-fold increase predicted from the RNAP partitioning. We therefore expect our results to provide a very good approximation even if there is a growth-rate dependence of macromolecular crowding.

Growth-Rate Dependence of the Ribosomal RNA Promoter P2. As mentioned, the question of whether P2 is a constitutive promoter is controversial in the literature. We therefore include a brief review of the experimental evidence for and against constitutive expression from P2 along with some comments. The claim that P2 is constitutive is mainly based on the following observations: (*i*) At slow growth, transcription from P2 has the same growth-rate dependence as transcription from other constitutive promoters (2). (*ii*) For any given growth rate, transcription from P2 is the same in strains with and without ppGpp and/or Fis, 2 regulators of the P1 promoter (13). Although these experiments

do clearly rule out strong regulation of P2, they are consistent with weak regulation of P2, in particular, because both the covariation of P2 with other constitutive promoters at low growth rates and the unchanged transcription activity of P2 in strains lacking Fis and/or ppGpp are only approximate (see Fig. S3 *A* and *B* and figures 1 and 2 of ref. 13). Furthermore, the data for the growth-rate dependence of transcription from constitutive promoters (2) is only consistent with a constitutive P2 if the other promoters become saturated with RNAPs at high growth rates and not if the growth-rate-dependent free RNAP concentration follows the relation predicted by our model as shown in Fig. 3.

Murray *et al.* (24, 25), on the other hand, have presented data in support of the claim that P2 is regulated in a growth-rate-dependent way. (*i*) In vitro, ppGpp decreased the transcription rate from P2 about 2-fold. Furthermore, ppGpp destabilized the open complex of promoter-bound RNAP (24, 25). However, it is not obvious that these in vitro experiments are representative of the in vivo situation. (*ii*) β-Galactosidase activity exhibits a pronounced growth-rate dependence when LacZ is expressed from a P2 promoter (24) (see also Fig. S3 *C*). This result is hard to interpret because enzyme activity under different growth conditions does not directly reflect the transcription rate, but may be also changed by a number of indirect effects such as the availability of ribosomes (which may affect the rate of translation initiation) and increased dilution of the protein due to faster growth. One, however, can compare the LacZ expression of different promoters under the same growth conditions as done in ref. 13. A comparison of the wild-type P2 promoter with a P2 mutants (figure 3 *C* and *G* of ref. 24; see also Fig. S3 *C* and *D*) shows that the activities of these promoters does not change in parallel over the studied range of growth rates, their ratio (mutant:wild type) decreases from 2.5 to 1.3 (Fig. S3 *C*). Because both promoters appear to be unsaturated with RNAPs, this means that at least one of them is regulated in some growth-rate-dependent way. (Other promoter mutants studied in ref. 17 are possibly saturated with RNAP and do not yield conclusive results.) Because in vitro transcription from the wild-type P2 promoter is affected by ppGpp (24, 25), this result is likely to indicate a growth-rate-dependent regulation of P2.

Growth-Rate Dependent Promoter Strength for the Average mRNA Promoter. To determine the strength of the average mRNA promoter $A_{\rm m}$ in the same way as that of the *rrn* promoters, information about the number $N_{\rm op}$ of operons or promoters is needed, but even without this information we can directly compute the effective promoter strength of the entire pool of mRNA promoters, $A_{\rm mRNA} = A_{\rm m}\, N_{\rm op}$. We found $A_{\rm mRNA} \approx 200\ (\mu{\rm M\ s})^{-1}$ with little dependence on growth rate (Fig. S6 *B*). This result has several possible interpretations: If the number of operons being transcribed at different growth rates remains rather constant, then the mRNA operons should not be strongly regulated. Alternatively, if more operons are transcribed at low growth rates (e.g., transporters and enzymes in biosynthetic pathways), then the decreases in the number of active operons at fast growth should be compensated by up-regulation of their transcription. At a growth rate of 1.5 doublings per hour, the number of different mRNA transcripts per cell is ≈600 (10), yielding an estimated strength $A_{\rm m}$ of $\approx 0.3\ (\mu{\rm M\ s})^{-1}$, which is much weaker than that of the *rrn* promoter.

1. Record MT, Reznikoff WS, Craig MA, McQuade KL, Schlax PJ (1996) Escherichia coli RNA polymerase (Eσ70), promoters, and the kinetics of the steps of transcription initiation. *Escherichia coli and Salmonella*, ed Neidhardt FC (ASM Press, Washington, DC), 2nd Ed, pp 792–820.
2. Liang ST, *et al.* (1999) Activities of constitutive promoters in Escherichia coli. *J Mol Biol* 292:19–37.
3. Reppas NB, Wade JT, Church GM, Struhl K (2006) The transition between transcriptional initiation and elongation in E-coli is highly variable and often rate limiting. *Mol Cell* 24:747–757.
4. Tadmor AD, Tlusty T (2008) A coarse-grained biophysical model of E. coli and its application to perturbation of the rRNA operon copy number. *Plos Comput Biol* 4:e1000038.
5. Bremer H, Dennis PP (1996) Modulation of chemical composition and other parameters of the cell by growth rate. *Escherichia coli and Salmonella*, ed Neidhardt FC (ASM Press, Washington, DC), 2nd Ed, pp 1553–1569.
6. Churchward G, Estiva E, Bremer H (1981) Growth Rate-dependent control of chromosome replication initiation in Escherichia Coli. *J Bacteriol* 145:1232–1238.
7. Rünzi W, Matzura H (1976) Distribution of RNA polymerase between cytoplasm and nucleoid in a strain of Escherichia coli. *Control of Ribosome Synthesis*, eds Kjeldgaard NO, Maaløe O (Munksgaard, Copenhagen), pp 115–116.
8. Shepherd N, Dennis P, Bremer H (2001) Cytoplasmic RNA polymerase in Escherichia coli. *J Bacteriol* 183:2527–2534.
9. Keseler IM, *et al.* (2005) EcoCyc: A comprehensive database resource for Escherichia coli. *Nucleic Acids Res* 33:D334–D337.
10. Neidhardt FC, Umbarger HE (1996) Chemical composition of Escherichia coli. *Escherichia coli and Salmonella*, ed Neidhardt FC (ASM Press, Washington DC), 2nd Ed, pp 13–16.
11. Salgado H, Moreno-Hagelsieb G, Smith TF, Collado-Vides J (2000) Operons in Escherichia coli: Genomic analyses and predictions. *Proc Natl Acad Sci USA* 97:6652–6657.
12. Xu L, *et al.* (2006) Average gene length is highly conserved in prokaryotes and eukaryotes and diverges only between the two kingdoms. *Mol Biol Evol* 23:1107–1108.
13. Zhang X, Dennis P, Ehrenberg M, Bremer H (2002) Kinetic properties of rrn promoters in Escherichia coli. *Biochimie* 84:981–996.
14. Klumpp S, Hwa T (2008) Stochasticity and traffic jams in the transcription of ribosomal RNA: Intriguing role of termination and antitermination. *Proc Natl Acad Sci USA* 105:18159–18164.
15. Saitoh T, Ishihama A (1977) Biosynthesis of RNA polymerase in Escherichia Coli. VI. Distribution of RNA-polymerase subunits between nucleoid and cytoplasm. *J Mol Biol* 115:403–416.
16. de Haseth PL, Lohman TM, Burgess RR, Record MT (1978) Nonspecific interactions of Escherichia-Coli RNA polymerase with native and denatured DNA: Differences in binding behavior of core and holoenzyme. *Biochemistry* 17:1612–1622.
17. Williams RC, Chamberlin MJ (1977) Electron microscope studies of transient complexes formed between Escherichia coli RNA polymerase holoenzyme and T7 DNA. *Proc Natl Acad Sci USA* 74:3740–3744.
18. Elf J, Li GW, Xie XS (2007) Probing transcription factor dynamics at the single-molecule level in a living cell. *Science* 316:1191–1194.
19. Ellis RJ (2001) Macromolecular crowding: obvious but underappreciated. *Trends Biochem Sci* 26:597–604.
20. Cayley S, Record MT (2004) Large changes in cytoplasmic biopolymer concentration with osmolality indicate that macromolecular crowding may regulate protein-DNA interactions and growth rate in osmotically stressed Escherichia coli K-12. *J Mol Recognit* 17:488–496.
21. Zimmerman SB, Trach SO (1991) Estimation of macromolecule concentrations and excluded volume effects for the cytoplasm of Escherichia Coli. *J Mol Biol* 222:599–620.
22. Elowitz MB, Surette MG, Wolf PE, Stock JB, Leibler S (1999) Protein mobility in the cytoplasm of Escherichia coli. *J Bacteriol* 181:197–203.
23. Donachie WD, Robinson AC (1987) Cell division: Parameter values and the process. *Escherichia coli and Salmonella typhimurium*, eds Neidhardt FC, *et al.* (ASM Press, Washington, DC), Vol 2, pp 1578–1592.
24. Murray HD, Appleman JA, Gourse RL (2003) Regulation of the Escherichia coli rrnB P2 promoter. *J Bacteriol* 185:28–34.
25. Murray HD, Gourse RL (2004) Unique roles of the rrn P2 rRNA promoters in Escherichia coli. *Mol Microbiol* 52:1375–1387.
26. Shepherd NS, Churchward G, Bremer H (1980) Synthesis and activity of ribonucleic acid polymerase in Escherichia Coli. *J Bacteriol* 141:1098–1108.
27. Engbaek F, Gross C, Burgess RR (1976) Quantitation of RNA polymerase subunits in Escherichia coli during exponential growth and after bacteriophage T4 infection. *Mol Gen Genet* 143:291–295.
28. Matzura H, Hansen BS, Zeuthen J (1973) Biosynthesis of beta and beta′ subunits of RNA polymerase in Escherichia coli. *J Mol Biol* 74:9–20.
29. Iwakura Y, Ito K, Ishihama A (1974) Biosynthesis of RNA polymerase in Escherichia coli. I. Control of RNA polymerase content at various growth rates. *Mol Gen Genet* 133:1–23.
30. Pedersen S, Bloch PL, Reeh S, Neidhardt FC (1978) Patterns of protein synthesis in Escherichia coli. Catalog of amount of 140 individual proteins at different growth rates. *Cell* 14:179–190.
31. Grigorova IL, Phleger NJ, Mutalik VK, Gross CA (2006) Insights into transcriptional regulation and sigma competition from an equilibrium model of RNA polymerase binding to DNA. *Proc Natl Acad Sci USA* 103:5332–5337.

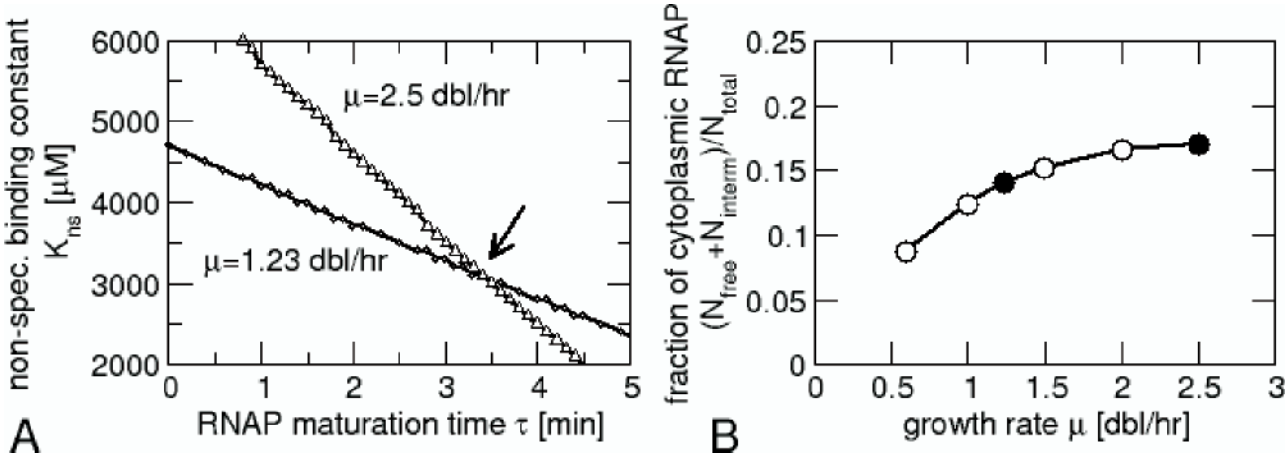

Fig. S1. Fit to cytoplasmic RNAP fraction from minicell data. The fraction of cytoplasmic RNAPs, i.e., free RNAPs and assembly intermediates, was determined for different choices of the two unknown parameters of our model, the dissociation constant K_{ns} for nonspecific RNAP-DNA binding and the RNAP maturation time τ. (*A*) Shown are parameter combinations that match the cytoplasmic RNAP fraction at growth rate of 1.23 doublings per hour [14% (7), black circles] and 2.5 doublings per hour [17% (8), triangles]. The intersection of the 2 curves determines the parameters K_{ns} and τ. (*B*) Predicted growth-rate dependence of the fraction of cytoplasmic RNAPs (line and open circles), together with the experimental data from refs. 7 and 8 (filled circles).

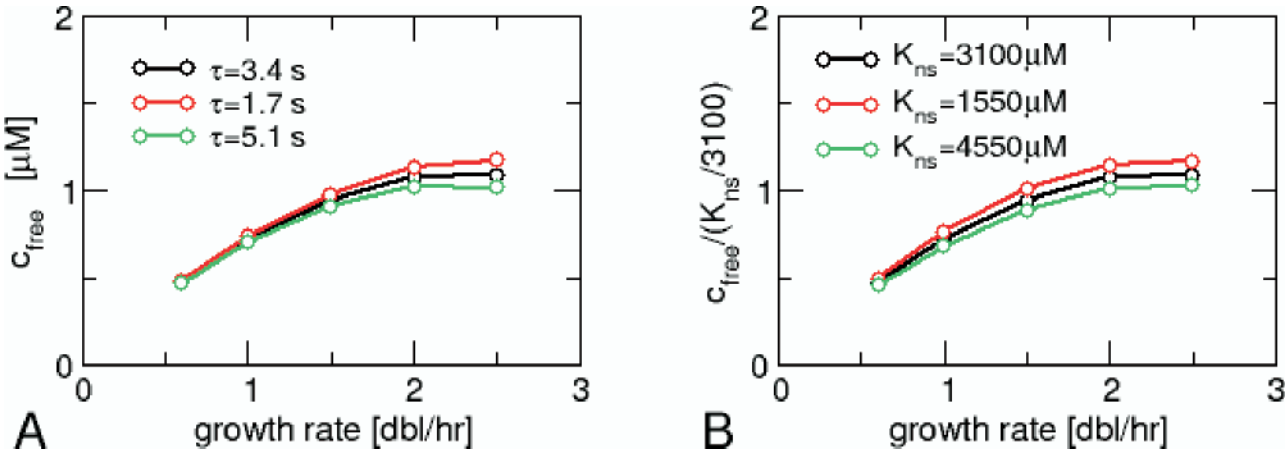

Fig. S2. Effect of the parameters τ and K_{ns} on the predicted free-RNAP concentration. (*A*) Increasing or decreasing the RNAP maturation time τ by 50% compared with the predicted value of 3.4 s has a very small effect on the predicted free-RNAP concentration c_{free}. (*B*) Increasing or decreasing the dissociation constant K_{ns} for nonspecific RNAP-DNA binding approximately rescales the free-RNAP concentration in a linear fashion.

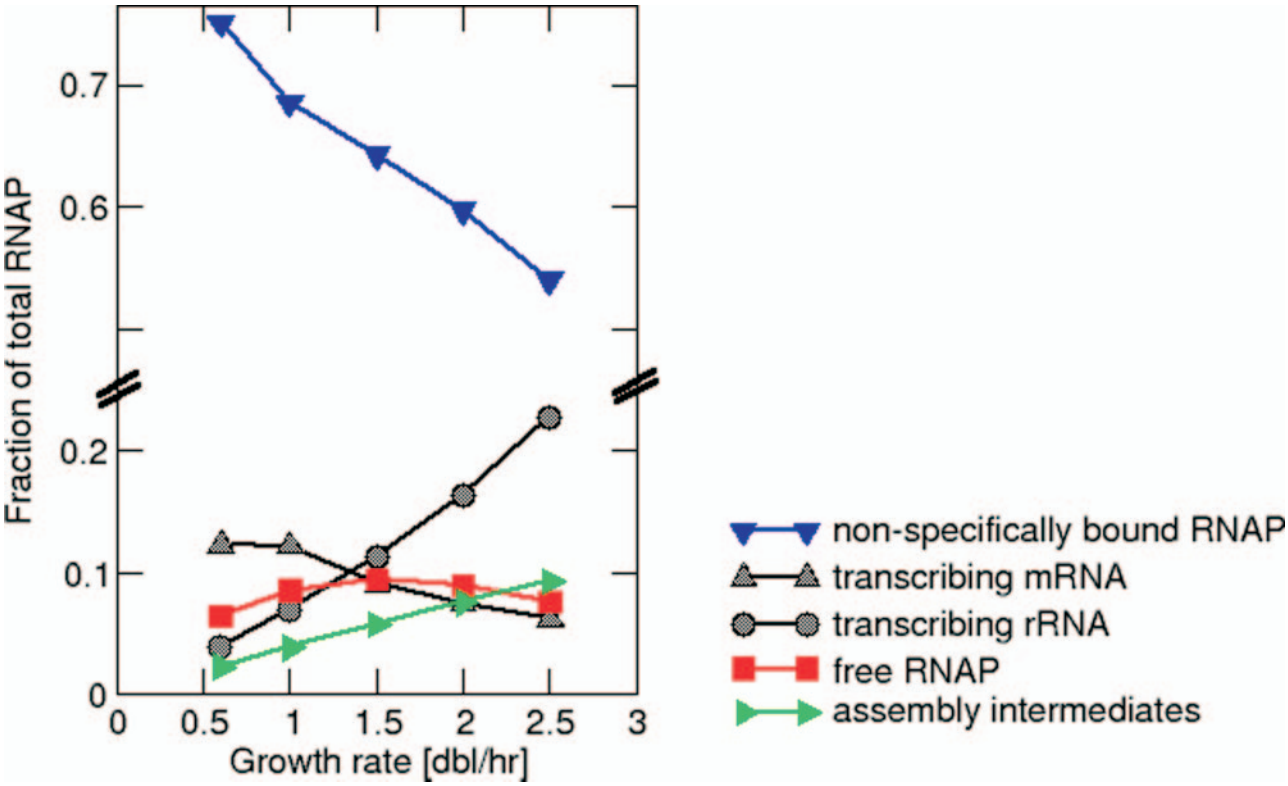

Fig. S3. Growth-rate-dependent partitioning of RNAPs. Fractions of the total number of RNAP in the different classes as functions of growth rates.

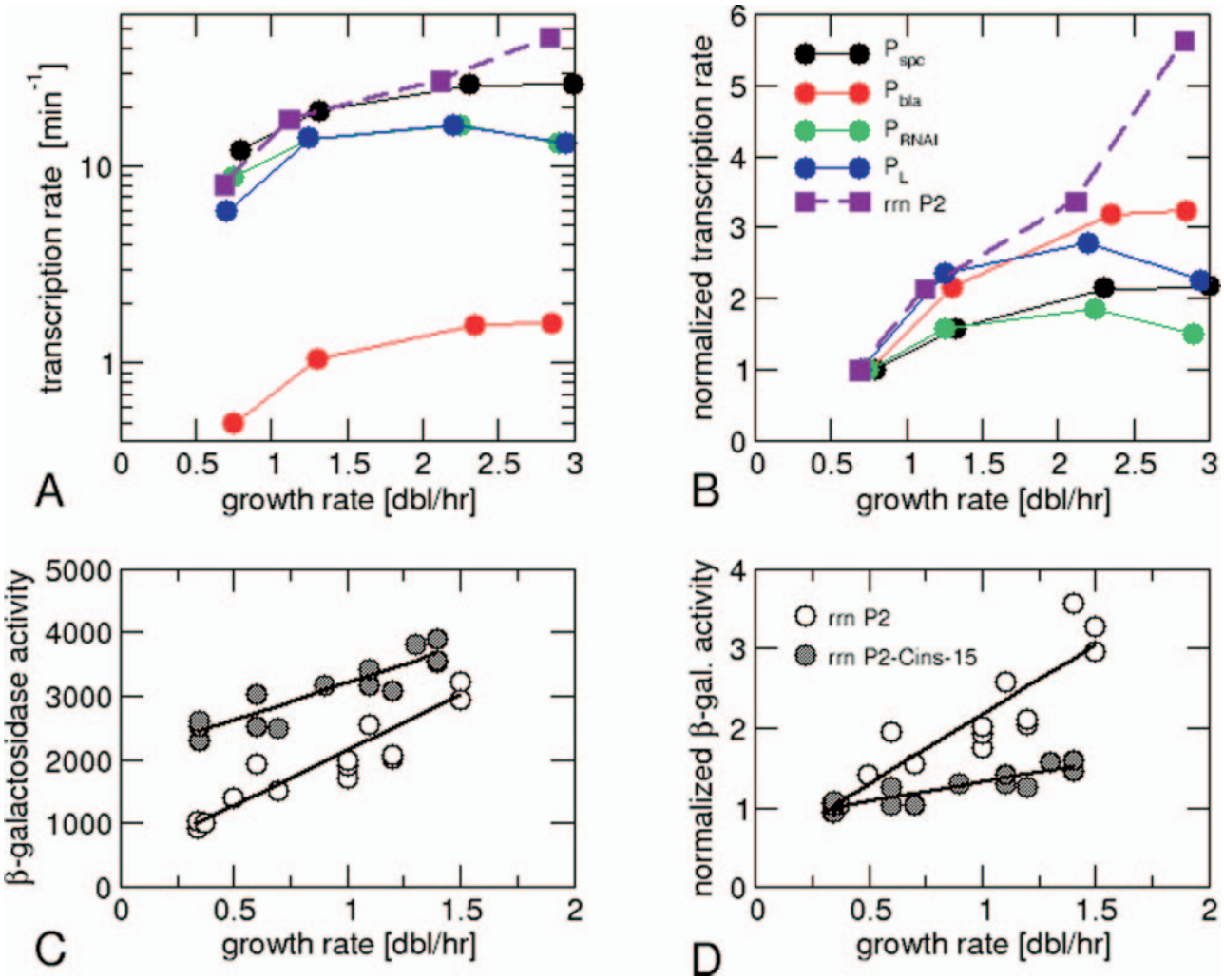

Fig. S4. Measurements of growth-rate-dependent promoter activities. (*A*) Promoter activities for promoters believed to be constitutive as reported in ref. 2. These promoters are the ribosomal protein promoter P_{spc}, the plasmid promoters P_{bla} and P_{RNAI}, the promoter P_L from phage λ and the *rrn* promoter P2. (*B*) The same data normalized to the value at the lowest growth rate. (*C*) β-Galactosidase activity obtained with LacZ expressed from the wild-type (−112 to + 7) rrn P2 promoter (filled symbols) and a P2 mutant (insertion of C at −15) from ref. 24. (*D*) The same data normalized to the value at the lowest growth rate.

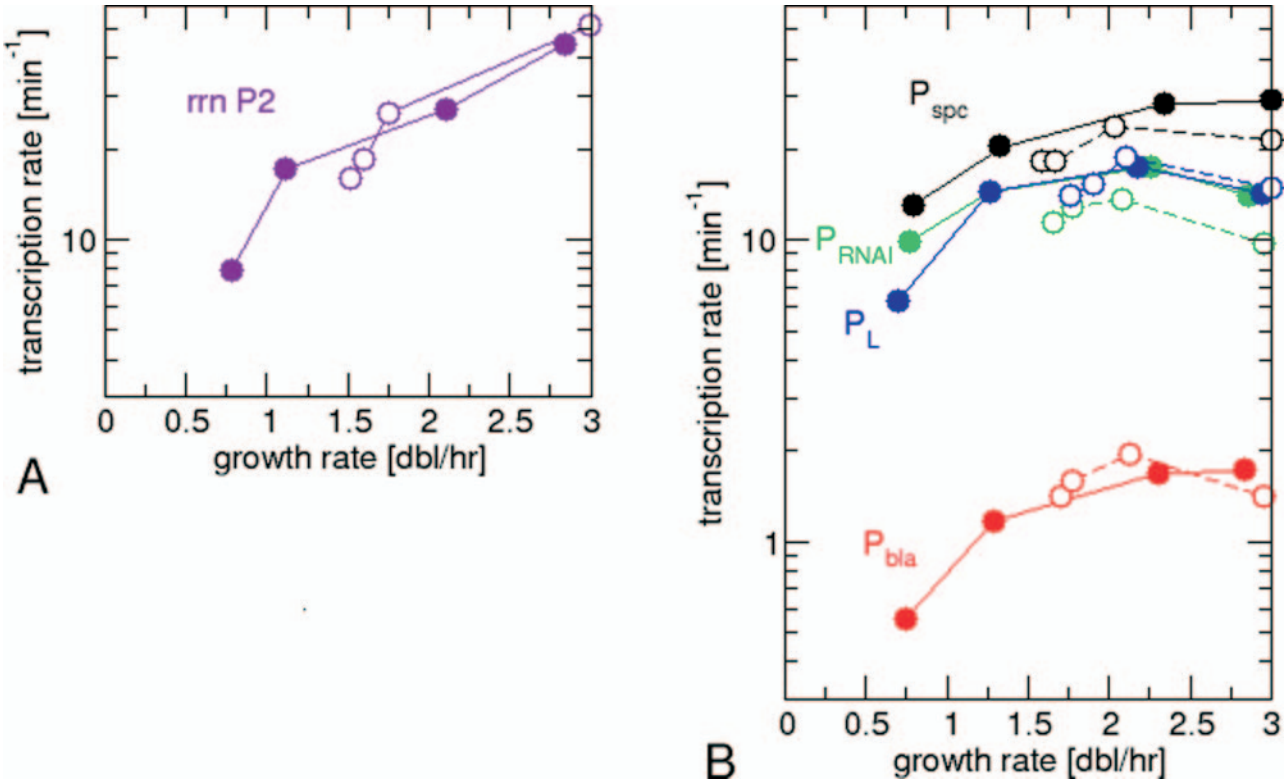

Fig. S5. Growth-rate dependence of transcription rates in wild-type and ppGpp-less cells. Filled symbols show transcription rates for the wild-type and open symbols those for a relaxed strain (ΔrelA ΔspoT) as measured by Liang *et al.* (2). (*A*) Transcription rates for the *rrn* promoter P2, taken from figures 3b and 3f of ref. 2. (*B*) Transcription rates for the constitutive promoters P_{spc}, P_{RNAI}, P_L, and P_{bla}, taken from figures 2a and 2b of ref. 2.

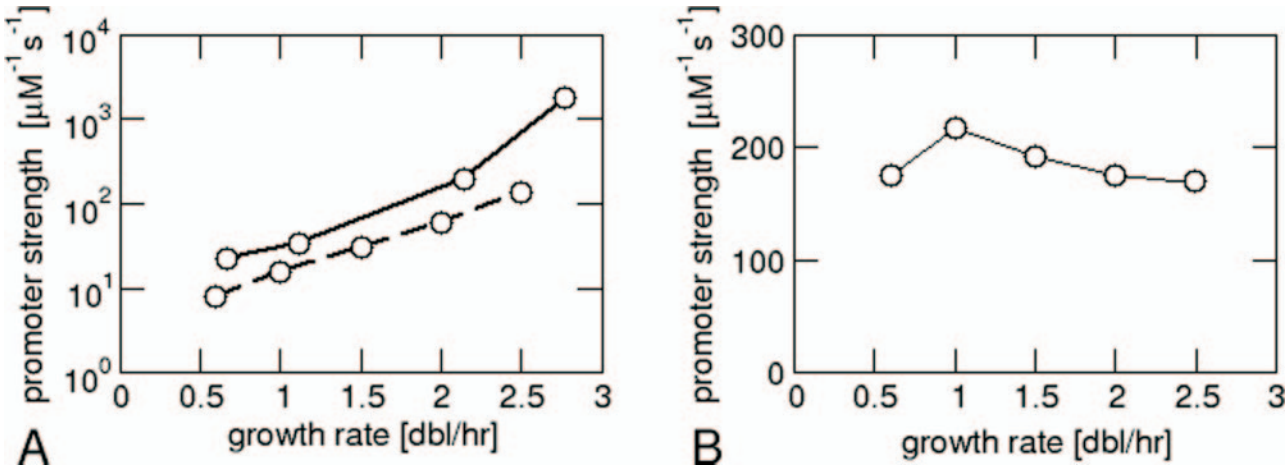

Fig. S6. Growth-rate dependence of promoter strengths. (*A*) Promoter strength A_r of the *rrn* P1-P2 promoter pair as obtained from the transcription rates given in ref. 5 (dashed line) and ref. 13 (solid line). (*B*) Effective promoter strength A_{mRNA} of the total pool of mRNA promoters.

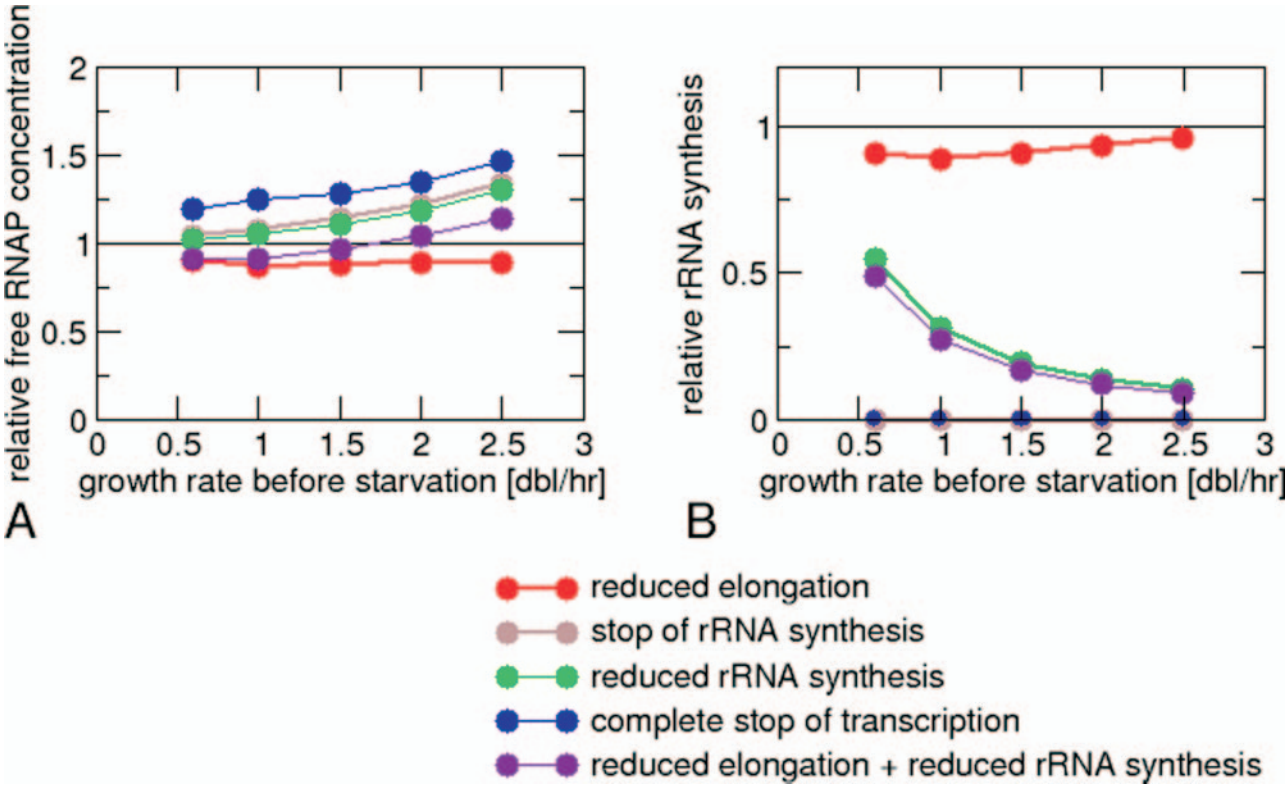

Fig. S7. Dependence of changes during the stringent response on the growth rate before starvation. (*A*) The free RNAP concentration during the stringent response relative to the concentration before starvation. (*B*) The relative transcription rate of rRNA. Note that in the case of reduced mRNA elongation (red), the reduction of rRNA synthesis is a consequence of the reduced free-RNAP concentration, whereas, in the other cases, the increase of the free RNAP concentration is a consequence of the reduction of rRNA transcription. The last scenario (violet) combines both effects, but shows that the reduction of rRNA synthesis dominates.

Table S1. Growth-rate-dependent parameters

Parameter	Symbol	Growth rate μ, doublings/h					Notes and references
		0.6	1.0	1.5	2.0	2.5	
Total number of RNAP molecules per cell	N_{total}	1,500	2,800	5,000	8,000	11,400	5*
DNA per cell (genome equivalents)	G_C	1.6	1.8	2.3	3.0	3.8	5
rrn operons per cell	N_{rrn}	12.4	15.1	20.0	26.9	35.9	5
Mass per cell, OD_{460} units/10^9 cells	M_C	0.85	1.49	2.5	3.7	5.0	5
Cell volume, μm^3	V_C	0.34	0.55	0.84	1.11	1.32	Calculated from M_C and the volumes measured in ref. 6†
mRNA elongation speed, nt/s	c_m	39	45	50	52	55	5
rRNA elongation speed, nt/s	c_r	85	85	85	85	85	5
mRNA synthesis rate per cell, 10^5 nt/min	r_m	4.3	9.2	13.7	18.7	23.4	5
rRNA synthesis rate per cell, 10^5 nt/min	r_r	3.0	9.9	29.0	66.4	132.5	5
Number of RNAPs transcribing mRNA per cell	N_m	184	341	457	599	709	Calculated as r_m/c_m
Number of RNAPs transcribing rRNA per cell	N_r	59	194	569	1,302	2,598	Calculated as r_r/c_r

*The numbers of total RNAPs per cell at different growth rates as given in ref. 5 and as used here are based on measurements from ref. 26, which are in good agreement with corresponding measurements from several other labs (27–30). A recent study, however, has reported considerably higher numbers of RNAPs per cell (31). All of these studies are based on measurements of the mass fraction of total protein that is RNAP, usually called α_P, from which the number of RNAPs per cell is obtained by multiplication with mass per cell. [More precisely, these experiments determine the amounts of the β and β' subunits of RNAP, as the α subunit is known to be present in excess (27, 29, 30)]. Comparison of the measured α_P values shows that all studies including ref. 31 agree on the growth-rate dependence of this value and that the discrepancy between ref. 31 and the older studies is due to a unusually large amount of total protein per cell in ref. 31, ≈3-fold larger than in the older studies.

†In ref. 6, the cell mass and volume was measured for growth rates of 1.3 doublings per hour and 2.14 doublings per hour, from these measurements, the mass per volume appears to increase slightly with growth rate, taken into account here by inter- and extrapolation. Larger values (≈1.5-fold) for the cell volume are given in ref. 23. We have also used these larger values in our calculation, and obtained very similar results (data not shown). In particular, we obtained almost the same prediction for the concentration of free RNAPs (which, in the larger volume, however, corresponds to a larger number of free RNAPs) and for the nonspecific dissociation constant, but a smaller maturation time (1.9 min), and thus a smaller number of immature RNAPs per cell.

Table S2. Growth-rate-independent parameters

Parameter	Symbol	Value	Notes and references
Length of mRNA operon, nt	L_m	3,000	see *SI Methods*
Length of rRNA operon, nt	L_r	6,500	Includes all tRNA genes; see *SI Methods*
Number of nonspecific binding sites per genome	g	4.6×10^6	From EcoCyc (9)
Dissociation constant for nonspecific binding, μM	K_{ns}	3,100	From fit of model to minicell data; see *SI Methods*
RNAP maturation time, min	τ	3.4	From fit of model to minicell data; see *SI Methods*